Journal of Environmental Management 380 (2025) 124918

Contents lists available at ScienceDirect

Journal of Environmental Management

journal homepage: www.elsevier.com/locate/jenvman

Research article

Metabolic response of *Zostera noltei* transplants in a historically contaminated ecosystem

V.H. Oliveira [a,*], D. Matos [b], A.I. Sousa [a], M. Dolbeth [c], B. Marques [a], A.I. Lillebø [a], M.E. Pereira [d], S. Díez [e], E. Figueira [b], J.P. Coelho [a]

[a] ECOMARE, CESAM - Centre for Environmental and Marine Studies, Department of Biology, University of Aveiro, Estrada do Porto de Pesca Costeira, 3830-565, Gafanha da Nazaré, Portugal
[b] CESAM - Centre for Environmental and Marine Studies, Department of Biology, University of Aveiro, Campus de Santiago, 3810-193, Aveiro, Portugal
[c] CIIMAR - Interdisciplinary Centre of Marine and Environmental Research, Novo Edifício Do Terminal de Cruzeiros Do Porto de Leixões, Avenida General Norton de Matos S/N, 4450-208, Matosinhos, Portugal
[d] LAQV-REQUIMTE, Department of Chemistry, University of Aveiro, Campus de Santiago, 3810-193, Aveiro, Portugal
[e] Environmental Chemistry Department, Institute of Environmental Assessment and Water Research, IDAEA-CSIC, E-08034, Barcelona, Spain

ARTICLE INFO

Keywords:
Seagrass
Contaminant
Antioxidant mechanisms
Recolonization
Monitoring protocol

ABSTRACT

In the midst of the UN Decade on Ecosystem Restoration and newly approved EU Nature Restoration Law, ecosystem restoration efforts have gained momentum. Still, monitoring tools and early warning protocols to evaluate restoration success are necessary. This study aimed to assess the suitability of using biochemical response parameters to evaluate *Z. noltei* tolerance to transplantation and various abiotic conditions (including metal(loid) concentrations) across different tissues and seasons, following restoration. The results indicate that the proposed monitoring strategy successfully highlighted the adaptation and acclimation phase of transplanted plants, as well as the tolerance to the conditions at the Transplant site by activating mechanisms to mitigate or reduce oxidative stress. The findings validate the use of biochemical response parameters as a measure of transplant success and early warning signal for plant maladjustment in the scope of ecosystem restoration actions in historically contaminated areas.

1. Introduction

Throughout the 20th century, estuarine and coastal ecosystems have experienced substantial degradation due to human activities such as urbanization, intensive agriculture, and industrialization (Kang et al., 2021; Salinas et al., 2020; Zhai et al., 2020). These disturbances have resulted in the loss of local fauna and flora, causing a decline in important/essential ecosystem services (Bashir et al., 2020; Beaumont et al., 2007). In response, there has been a growing international effort to restore degraded ecosystems, driven by policies like the Convention on Biological Diversity, the European Green Deal, the United Nations Decade for Ecosystem Restoration (2021–2030), and the EU Nature Restoration Law. Among the various restoration strategies (physical, chemical, and biological), biological remediation stands out for its cost-effectiveness and environmentally friendly nature (Oliveira et al., 2024). Moreover, in cases where contaminants are present in sediments, this method is capable of transforming organic contaminants into harmless substances or immobilizing them (Hamad et al., 2021; Karimi et al., 2022; Oliveira et al., 2023; Rostami and Azhdarpoor, 2019; Vishwakarma et al., 2020; Zhang et al., 2020). Furthermore, biological remediation, particularly using plants, not only helps to restore ecosystems but also contributes to mitigating global warming through the sequestration of atmospheric carbon, known as blue carbon (Brown et al., 2021; Sousa et al., 2017).

One of the most promising approaches to ecosystem restoration and rehabilitation involves the use of seagrasses, which play a vital role in restoring and rehabilitating degraded coastal ecosystems (Orth et al., 2020). Seagrasses sequester carbon, provide habitat for numerous species and enhance local biodiversity (Crespo et al., 2023). They also improve water quality and reduce drag force by bending in the direction of water flow, which decreases flow velocity throughout the canopy (Morris et al., 2008; Verduin and Backhaus, 2000). This action creates more favourable conditions for fauna development and helps reduce sediment erosion (Brun et al., 2021; Jiménez-Ramos et al., 2019; Morris

* Corresponding author.
E-mail address: vitor.hugo.oliveira@ua.pt (V.H. Oliveira).

https://doi.org/10.1016/j.jenvman.2025.124918
Received 6 January 2025; Received in revised form 3 March 2025; Accepted 7 March 2025
Available online 12 March 2025
0301-4797/© 2025 The Authors. Published by Elsevier Ltd. This is an open access article under the CC BY-NC license (http://creativecommons.org/licenses/by-nc/4.0/).

et al., 2008; Unsworth et al., 2022; Valdez et al., 2020; Wahyudi et al., 2020).

Despite their ecological benefits, the implementation of seagrass restoration in new and contaminated sites poses challenges. Seagrasses are highly sensitive to changes in atmospheric conditions, physico-chemical parameters and contaminant exposure. For example, Touchette and Burkholder (2000) found that elevated temperatures generally accelerate photosynthesis and respiration up to an optimal threshold, beyond which the regulation of antioxidant enzymes may become disrupted. Additionally, studies by Piro et al. (2015) and Sandoval-Gil et al. (2023) have reported that seagrasses employ various mechanisms to cope with salinity fluctuations, such as modulating carbon metabolism (e.g., reducing RuBisCO expression while increasing glycolytic enzyme levels), enhancing vacuolar Na^+ sequestration, and adjusting osmotic balance.

Regarding contaminant exposure, seagrasses exhibit varied responses. Research on species such as *Halophila beccarii*, *Zostera marina*, and *Zostera muelleri* indicates that exposure to metals such as copper and cadmium decreases photosynthetic efficiency and increases the production of reactive oxygen species (ROS), that can lead to oxidative stress by damaging proteins, lipids, and DNA (Buapet et al., 2019; Chen and Qiu, 2024; Greco et al., 2019). Moreover, metals such as lead can reduce seed germination, inhibit growth, and decrease biomass (Brackup and Capone, 1985; Li et al., 2023). In response, seagrasses often upregulate antioxidant enzymes, such as superoxide dismutase, catalase, and glutathione peroxidase, to mitigate oxidative damage (Buapet et al., 2019; Chen and Qiu, 2024; Lin et al., 2016). This adaptive response suggests that certain species may tolerate high contaminant levels without exhibiting biochemical damage, suggesting their potential for phytoremediation, as observed in the seagrass species *Posidonia oceanica*, *Cymodocea nodosa*, *Halophila stipulacea*, and *Zostera marina* (Bonanno and Orlando-Bonaca, 2017; Brix et al., 1983; Lee et al., 2019).

Building on evidence that different seagrass species exhibit distinct physiological responses to contaminants, and with the primary goal of restoring a historically contaminated area with varying metal(loid) concentrations (e.g., arsenic, cadmium, copper, and mercury) in the Aveiro Lagoon, Portugal, laboratory studies were previously conducted by Fonte et al. (2023) and Oliveira et al. (2025b). These controlled experiments focused on understanding the biochemical and physiological responses of the native species *Zostera noltei* to contaminants present in an inner bay of the Aveiro Lagoon, known as Laranjo Bay. The studies aimed to fill critical gaps in knowledge regarding the species' responses to different contaminants, with results showing that contaminant presence did not compromise seasonal variations in biomass, coverage area, or key biochemical and physiological parameters (e.g., photosynthetic efficiency).

Based on these promising results, a pilot transplant of *Z. noltei* was initiated in Laranjo Bay as a Nature-based Solution (NbS) for ecological restoration (Crespo et al., 2023; Oliveira et al., 2023). The transplant's success was monitored over time by evaluating physiological indicators such as biomass, coverage area, and photosynthetic efficiency (Oliveira et al., 2025a). Additionally, biochemical markers (including energy budgets and antioxidant enzyme activities) were analysed as early-warning indicators of plant stress. These biochemical responses provide valuable insights into plant acclimation during the early transplantation phase and its potential adaptations to abiotic stressors over time. Moreover, they help detect signs of maladaptation before visible symptoms arise, enabling timely interventions to prevent project failure and enhance the long-term success of restoration in contaminated ecosystems (Blanco-Murillo et al., 2024; Griffiths et al., 2020; Kerninon et al., 2021).

To ensure the effectiveness of the restoration efforts, the following specific objectives were established: 1) characterize the contaminant pools present in the sediments from the Donor (reference site) and Transplant site (contaminated site) over time; 2) monitor the acclimation process of transplanted *Z. noltei* plants to the conditions at the Transplant site; 3) measure energy budgets and oxidative stress levels across different tissues and seasons; and 4) validate the use of biochemical response parameters as a measure of transplant success and early warning signal for plant maladjustment.

2. Methodology

2.1. Site description

The Aveiro Lagoon, situated in Portugal, is a shallow coastal lagoon renowned for its intertidal zones and intricate network of four primary channels shaped by semidiurnal tides, spanning approximately 45 km.

Owing to its strategic location, the Aveiro Lagoon has been subject to substantial industrialization, resulting in challenges stemming from both direct and indirect discharge of domestic and industrial waste into its waters. The most pronounced environmental impacts unfolded during the latter half of the 20th century (Oliveira et al., 2018), notably attributed to the periodic release of industrial effluents, primarily originating from a chlor-alkali factory situated within the Estarreja chemical complex (Oliveira et al., 2022; Válega et al., 2008a). These effluents were discharged into the upstream region of the lagoon, specifically Laranjo Bay, resulting in a well-defined metal(loid)s contamination gradient (Coelho et al., 2005; Ereira et al., 2015; Stoichev et al., 2019, 2020) within this enclosed bay (Fig. 1A). Consequent to the discharge of contaminants, a discernible decline in local flora and fauna has been documented (García-Seoane et al., 2016; Nunes et al., 2008; Válega et al., 2008b). Nonetheless, in recent decades, cessation of such discharges has spurred a gradual natural recovery of the ecosystem, characterized by the gradual resurgence of halophytic plants within Laranjo Bay, particularly in its upper intertidal zones (Figueira et al., 2012; Oliveira et al., 2018; Válega et al., 2008b).

To accelerate the restoration of the area, mainly in the central intertidal area, a seagrass (*Z. noltei*) transplant initiative was undertaken in the summer of 2020, employing the patch transplant methodology (Oliveira et al., 2025a). Accordingly to Costa et al. (2022), this approach facilitates the transfer of seagrass plants and sediment, preserving their roots, rhizomes, and leaves, while minimizing disturbance to the Donor meadow. Patches of *Z. noltei* were harvested from a Donor meadow (Fig. 1B) situated 3 km downstream from the transplant zone and transplanted within Laranjo Bay, utilizing a chessboard pattern to facilitate expansion in all directions (Fig. 1C) (Oliveira et al., 2025a).

2.2. Sampling method

To assess the adaptability and biochemical response of *Z. noltei* to the transplant process and varying abiotic conditions, including sediment contamination found in Laranjo Bay, energy budgets and oxidative stress levels were examined in aboveground (leaves) and belowground (roots and rhizomes) tissues seasonally from summer 2020 (the transplant moment) through autumn 2021 as early-warning indicators.

Sampling was conducted in the Donor Meadow [DM] (Fig. 1B) and the Transplant Meadow [TM] (Fig. 1C). The DM served as a control/reference area, providing reference values as it hosted a well-established and stable meadow of *Z. noltei* prior to the transplant (Crespo et al., 2023). In each season, five cores of *Z. noltei* (8 cm deep, 15 cm diameter) were randomly collected from each meadow at low tide, except for the first season (summer 2020), in which sampling was conducted solely in DM due to the transplanting that took place on that day into the TM site. Upon collection, the cores were placed in plastic bags, stored in a cooler for transportation and processed in the laboratory. Plant biomass was separated from the sediments, and the sediment associated with the plant cores was divided into two aliquots. One aliquot was freeze-dried, and subsamples were taken for metal(loid) concentration analysis. The other aliquot was dried, disaggregated, and homogenized for the analysis of organic matter content and the fine fraction (<63 μm). Regarding biomass, once separated from the sediments, the biomass was divided

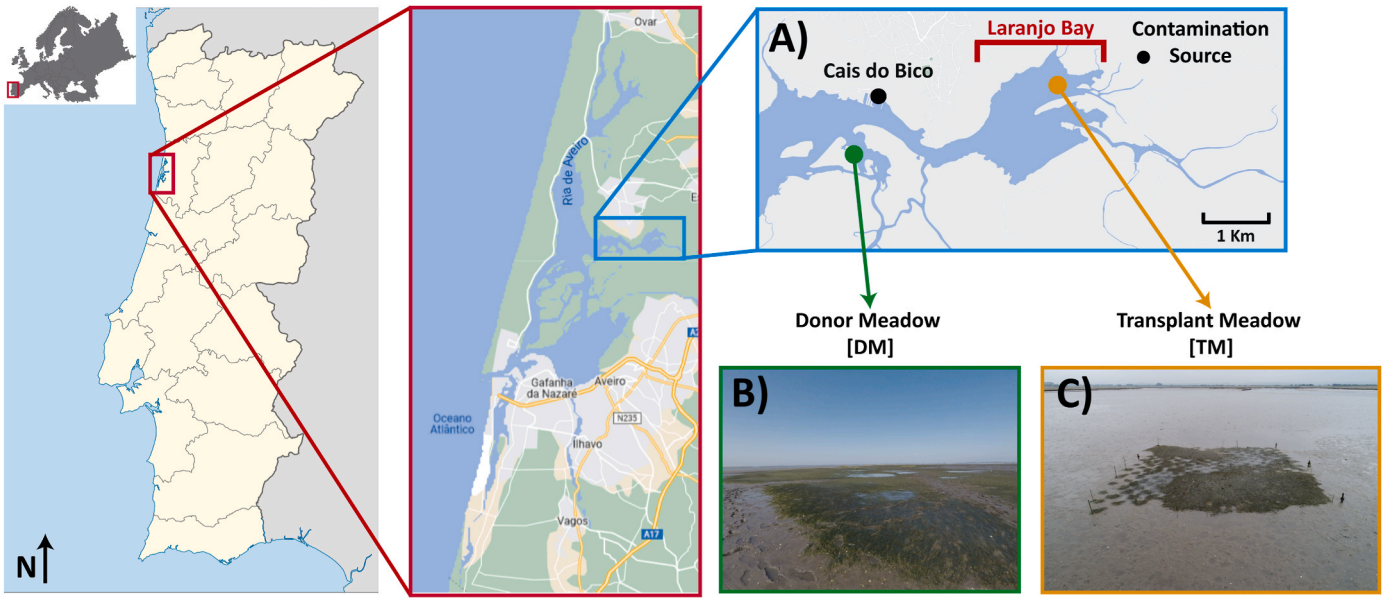

Fig. 1. Schematic plan of the Aveiro Lagoon and Laranjo Bay (A), showing the locations of the sampling sites for the *Zostera noltei* Donor Meadow (B) and the Transplant Meadow (C).

into living aboveground and belowground tissues. These tissues were gently washed with distilled water to remove any remaining sediment particles, then freeze-dried for at least 48 h using a Unicryo MC-4 L-60 C freeze-dryer and subsequently stored at −80 °C until biochemical analysis.

During the study period, the temperature and light intensity were continuously monitored every hour by two HOBO sensors (HOBO MX2202 Temp/Light) installed in the field. The total precipitation data (monthly averages) were obtained from INE (Instituto Nacional de Estatística).

2.3. Sediment characterization

The organic matter content was determined by loss on ignition (4 h at 500 °C), and the fine fraction of the sediments was determined by wet sieving following the methodology described in Oliveira et al. (2018).

Total mercury (Hg) concentrations in sediment samples were measured using a LECO AMA-254 Advanced Mercury Analyzer, following the method described by Costley et al. (2000). The performance of the LECO AMA-254 was verified daily through the analysis of Certified Reference Materials (CRM) with similar matrices, both at the beginning and at the end of the day. Recovery rates for BCR-277R (97–113%, n = 10) were within their respective confidence intervals. Samples were always analysed in at least triplicate, with a coefficient of variation lower than 10%.

Arsenic (As), cadmium (Cd), copper (Cu), nickel (Ni), lead (Pb), tin (Sn), titanium (Ti), uranium (U), and zinc (Zn) concentrations were determined using Inductively Coupled Plasma Mass Spectrometry (ICP-MS, Thermo X Series). These metal(loid)s concentrations in sediment samples were determined according to the US EPA 3051 protocol. Similar to Hg quantification, the performance of the ICP-MS was verified daily. To ensure the quality and reliability of the results, parallel blank and certified reference material (ERM-CC141 and BCR-143R) digestions were performed to monitor and control potential contaminations. The recovery rates achieved ranged from 96% to 116% for both CRMs.

2.4. Biochemical parameters

2.4.1. Extraction procedures

For biochemical analysis, aboveground and belowground tissues were divided into approximately 100 mg portions of freeze-dried tissue to assess energy consumption (Electron Transport System), available energy (soluble carbohydrates and insoluble carbohydrates (starch)), oxidative damage (lipid peroxidation and protein carbonylation), and antioxidant response (activity of antioxidant enzymes). Each sample was homogenized in 200 μL of specific buffers tailored for each analysis using an ultrasonic probe for 15 s at 0.5 cycles.

For the assessment of the Electron Transport System (ETS), homogenization was carried out in 0.1M Tris-HCl buffer (pH 8.5) containing 15% (w/v) Poly Vinyl Pyrrolidone, 153 μM magnesium sulphate, and 0.2% (v/v) Triton X-100. The homogenate was then centrifuged at 4 °C for 20 min at 3000 g.

To evaluate soluble carbohydrates (sCH) and starch (ST), carbohydrates were extracted with potassium phosphate buffer (0.1 M dipotassium phosphate; 0.1 M potassium dihydrogen phosphate; 5 mM EDTA; 0.1% (v/v) Triton X-100; pH 7.5) using a mortar and pestle, followed by centrifugation at 10,000*g* for 10 min. The supernatant was used to determine soluble carbohydrates while the pellet was incubated at 95 °C for 30 min. After cooling in an ice bath, samples were centrifuged at 10,000 g for 4 min, and the supernatant was used to quantify starch.

For lipid peroxidation (LPO), supernatants were extracted using 20% (v/v) trichloroacetic acid.

To quantify reduced (GSH) and oxidized (GSSG) glutathione, homogenization was performed using 0.6% sulfosalicylic acid in potassium phosphate buffer (0.1 M dipotassium phosphate; 0.1 M potassium dihydrogen phosphate; 5 mM EDTA; 0.1% (v/v) Triton X-100; pH 7.5). Subsequently, the samples were centrifuged at 10,000 g for 10 min at 4 °C.

The remaining parameters such as protein carbonylation (PC), superoxide dismutase (SOD), catalase (CAT), glutathione peroxidase (GPx), glutathione reductase (GR), ascorbate peroxidase (APX), and glutathione S-transferases (GST) were determined in samples homogenized with phosphate buffer (50 mM potassium dihydrogen phosphate; 50 mM potassium phosphate dibasic; 1 mM ethylenediamine tetraacetic acid disodium salt dihydrate; 1% (v/v) Triton X-100; 1 mM dithiothreitol), followed by centrifugation at 10,000*g* for 10 min at 4 °C.

For all biochemical parameters, the supernatant was separated from the pellet after centrifugation, and either used immediately or stored at −80 °C until further use.

2.4.2. Soluble protein content

The soluble protein content (PROT) was determined using the method outlined by Robinson and Hogden (1940). Bovine serum albumin (BSA) served as the standard, and absorbance was measured at 540 nm. Results were expressed as mg of soluble protein per g of dry weight (DW).

2.4.3. Electron transport system activity

The electron transport system (ETS) was determined using the protocol described by De Coen and Janssen (1997). In this method, the measurement of dehydrogenase activity is based on the reduction, during electron flow, of the tetrazolium dye INT (p-IodoNitroTetrazolium) that turns purple upon reduction. The amount of formazan formed was calculated using the molar extinction coefficient for formazan ($\mathfrak{E} = 15{,}900\ M^{-1}\ cm^{-1}$). Electron transport system activity was read at 490 nm for 10 min, and results were expressed as $\mu mol\ min^{-1}\ g^{-1}$ DW.

2.4.4. Energy reserves

Soluble carbohydrates (sCH) and starch (ST) were determined as measurements of the energy reserves, according to the method of DuBois et al. (1956). Quantification was based on the amount of colour produced at a constant phenol concentration that is proportional to the amount of sugar present. Glucose was used as the standard, and absorbance was read at 492 nm. Results were expressed in $mg\ g^{-1}$ DW.

2.4.5. Oxidative damage

Lipid peroxidation (LPO) and proteins carbonylation (PC) were determined using the protocols described by Buege and Aust (1978) and Udenigwe et al. (2016), respectively. The measurement of LPO was performed by quantification of thiobarbituric acid reactive substances and was measured at 532 nm ($\mathfrak{E} = 156{,}000\ M^{-1}\ cm^{-1}$). The amount of PC was determined by the quantification of carbonyl groups, through reaction with 2,4-dinitrophenylhydrazine and was measured at 450 nm ($\mathfrak{E} = 22{,}308\ M^{-1}\ cm^{-1}$). Both results were expressed in $\mu mol\ g^{-1}$ DW.

2.4.6. Antioxidant response

Superoxide dismutase activity was determined according to the method outlined by Beauchamp and Fridovich (1971), measuring the conversion of nitro blue tetrazolium (NBT) by superoxide radicals into NBT diformazan at 560 nm. Catalase activity was assessed following the protocol of Johansson and Håkan Borg (1988), where formaldehyde formation in reaction with Purpald produces a coloured product that absorbs light at 540 nm. Ascorbate peroxidase activity was determined using the method described by Nakano et al. (1981), measuring the oxidation of ascorbate at 290 nm ($\mathfrak{E} = 2.8\ mM^{-1}\ cm^{-1}$). Glutathione peroxidase activity was determined according to Paglia and Valentine (1967), monitoring the oxidation of NADPH at 340 nm ($\mathfrak{E} = 6220\ M^{-1}\ cm^{-1}$). Reduced (GSH) and oxidized (GSSG) glutathione were determined using the method of Rahman et al. (2007), using reduced and oxidized glutathione standards (0–90 μmol/L), with readings taken at 412 nm. Glutathione reductase activity was determined following the protocol of Carlberg and Mannervik (1985), based on the oxidation of NADPH at 340 nm ($\mathfrak{E} = 6220\ M^{-1}\ cm^{-1}$). Glutathione S-transferases activity was assessed using the method of Habig et al. (1974), measuring the increment at 340 nm ($\varepsilon = 9600\ M^{-1}\ cm^{-1}$) resulting from the formation of a thioether (catalyse the conjugation of the substrate 1-chloro-2,4-dinitrobenzene (CDNB) with glutathione). The activity of all the enzymes was expressed in $\mu mol\ min^{-1}\ g^{-1}$ DW.

2.5. Statistical analysis

All results were statistically tested using the permutation multivariate analysis of variance (PERMANOVA), considering a 2-way crossed design. The factors were Site (Donor meadow and Transplant meadow) and Time (summer 2020 [SUM 20]; autumn 2020 [AUT 20]; winter 2020 [WIN 20]; spring 2021 [SPR 21]; summer 2021 [SUM 21]; autumn 2021 [AUT 21]). Prior to the PERMANOVA, each factor was tested for its dispersion around the centroid using the PERMDISP analysis. All analyses were done with the PRIMER v6 software with PERMANOVA + add-on (Anderson et al., 2008). Significant differences were assigned for a p-value ≤ 0.05.

3. Results

3.1. Sediment characteristics

Significant differences in sediment characteristics were observed between the DM and the TM sites (Table 1). Sediments from the DM site consistently exhibited a higher percentage of organic matter and fine fraction compared to those from the TM site, in all time periods corresponding to different seasons. Regarding metal(loid)s, concentrations of As, Cd, Cu, Hg, and Zn were higher in sediments collected from the TM site, which is closer to the contamination source (Fig. 1A). In contrast, the remaining metal(loid)s (Ni, Pb, Sn, Ti, and U) tended to exhibit similar concentrations between the two study sites or were found in higher concentrations in the DM site. Seasonal variations in sediment characteristics were also evident. However, the PERMADISP revealed significant differences for Time due to the scattering of the data around the group centroids.

3.2. Atmospheric conditions

Atmospheric conditions varied from season to season (Table 2). The lowest temperatures and light intensities were recorded in the winter of 2020, with average values of 18 ± 5 °C and 10,043 ± 7499 Lum m^{-2}, respectively. The highest values were recorded in the summer, with the summer of 2020 being slightly warmer and having higher light intensities than the summer of 2021. Regarding total precipitation, the highest rainfall occurred in the autumn of 2020 (132 ± 49 mm), while the lowest was in the summer of 2020 (25 ± 22 mm).

3.3. Biochemical response of Zostera noltei

The biochemical results from different sampling periods are presented graphically in Figs. 2–4. All significant terms related to various fouling biochemical parameters for both belowground and aboveground tissues are detailed in Supplementary Table 1 (Supplementary Material).

3.3.1. Energy budgets

Significant differences in energy budgets (Fig. 2) were observed across meadows and over time (Supplementary Table 1). Between the DM and TM meadows, notable differences were found in belowground tissue, where ETS activity tended to be higher in TM, and in aboveground tissue, where ST levels were generally lower in TM.

Regarding temporal variations, nearly all energy parameters showed significant changes over time, except for PROT content in belowground tissue. In aboveground tissue, PROT content was higher during the spring and summer sampling periods. ETS activity, sCH levels, and ST levels showed differences over time in both tissues, generally presenting lower values during winter. The highest values depended on the tissue type and parameter. For instance, in aboveground tissue, a slight increase in ETS activity and energy reserves (such as sCH and ST) was noted in summer, whereas for the belowground tissue, ETS activity and ST levels increased earlier, starting in spring and remaining elevated throughout spring, summer, and autumn.

3.3.2. Antioxidant responses and oxidative damage

Antioxidant responses (Fig. 3) varied between meadows, with significant differences in belowground tissue observed only for CAT, GPx, and GSSG, where higher activity/level were generally found in the TM meadow. In aboveground tissue, differences between meadows were

Table 1
Organic matter (%), fine fraction (%) and metal(loid)s concentrations (mg kg^{-1}) in surface sediments at the Donor and Transplant meadows over time. Values are presented as means ± standard deviation of 5 replicates. Superscript letters indicate statistically significant differences between times at the 95% confidence level. Asterisk (*) denotes significant differences between meadows (DM vs. TM) for the same time.

			Time					
			SUM 20	AUT 20	WIN 20	SPR 21	SUM 21	AUT 21
Organic Matter		**DM**	9.6 ± 0.5 $^{(a)}$ *	8.6 ± 0.3 $^{(b)}$ *	9.1 ± 0.5 $^{(c,d)}$ *	8.7 ± 0.4 $^{(b,d)}$ *	10 ± 0 $^{(e)}$ *	9.0 ± 0.6 $^{(b,d)}$ *
		TM	5.3 ± 0.7 $^{(a)}$ *	6.1 ± 0.2 $^{(a)}$ *	5.8 ± 0.8 $^{(a)}$ *	6.4 ± 1.1 $^{(a)}$ *	5.9 ± 1.2 $^{(a)}$ *	6.2 ± 0.8 $^{(a)}$ *
Fine Fraction		**DM**	19 ± 2 $^{(a)}$	24 ± 3 $^{(b)}$	31 ± 2 $^{(c)}$ *	27 ± 4 $^{(d)}$ *	23 ± 2 $^{(b)}$	23 ± 1 $^{(b)}$
		TM	18 ± 3 $^{(a)}$	22 ± 2 $^{(b,c)}$	23 ± 0 $^{(c)}$ *	21 ± 2 $^{(b)}$ *	21 ± 2 $^{(b)}$	21 ± 2 $^{(b)}$
Metal(loid)s	**[As]**	**DM**	21 ± 4 $^{(a,b,c)}$ *	20 ± 0 $^{(a)}$ *	19 ± 1 $^{(b)}$ *	20 ± 1 $^{(a)}$ *	20 ± 1 $^{(a)}$ *	21 ± 0 $^{(c)}$ *
		TM	24 ± 1 $^{(a)}$ *	26 ± 1 $^{(b)}$ *	24 ± 1 $^{(a)}$ *	24 ± 1 $^{(a)}$ *	24 ± 0 $^{(a)}$ *	25 ± 1 $^{(a,b)}$ *
	[Cd]	**DM**	0.40 ± 0.04 $^{(a)}$ *	0.34 ± 0.01 $^{(b)}$ *	0.35 ± 0.02 $^{(b,c)}$ *	0.38 ± 0.02 $^{(a)}$	0.34 ± 0.01 $^{(b)}$ *	0.37 ± 0.02 $^{(a,c)}$ *
		TM	0.43 ± 0.02 $^{(a)}$ *	0.44 ± 0.03 $^{(a)}$ *	0.40 ± 0.03 $^{(b,c)}$ *	0.36 ± 0.06 $^{(b)}$	0.40 ± 0.06 $^{(a,b,c)}$ *	0.41 ± 0.02 $^{(c)}$ *
	[Cu]	**DM**	20 ± 2 $^{(a)}$	19 ± 0 $^{(b)}$ *	18 ± 0 $^{(c)}$ *	19 ± 1 $^{(b)}$ *	18 ± 0 $^{(c)}$ *	19 ± 1 $^{(a,b)}$ *
		TM	20 ± 0 $^{(a)}$	21 ± 1 $^{(b)}$ *	20 ± 1 $^{(c)}$ *	21 ± 2 $^{(a,b,c)}$ *	19 ± 1 $^{(c)}$ *	21 ± 1 $^{(b)}$ *
	[Hg]	**DM**	0.71 ± 0.08 $^{(a,c)}$ *	0.75 ± 0.20 $^{(a,c)}$ *	0.66 ± 0.01 $^{(a,b)}$ *	0.70 ± 0.03 $^{(c)}$ *	0.55 ± 0.21 $^{(b)}$ *	0.59 ± 0.15 $^{(b)}$ *
		TM	1.8 ± 0.5 $^{(a)}$ *	2.8 ± 0.5 $^{(b)}$ *	1.4 ± 0.2 $^{(a)}$ *	2.4 ± 0.3 $^{(b)}$ *	1.9 ± 0.4 $^{(a)}$ *	2.5 ± 0.2 $^{(b)}$ *
	[Ni]	**DM**	18 ± 2 $^{(a)}$ *	16 ± 0 $^{(b)}$ *	16 ± 0 $^{(b)}$ *	16 ± 1 $^{(c)}$ *	16 ± 0 $^{(c)}$ *	17 ± 2 $^{(a,c)}$ *
		TM	13 ± 0 $^{(a)}$ *	14 ± 1 $^{(b)}$ *	13 ± 1 $^{(c)}$ *	14 ± 2 $^{(b,c)}$ *	14 ± 1 $^{(b,c)}$ *	15 ± 1 $^{(b)}$ *
	[Pb]	**DM**	27 ± 3 $^{(a)}$ *	24 ± 0 $^{(b)}$	23 ± 1 $^{(c)}$ *	24 ± 1 $^{(b)}$ *	23 ± 0 $^{(d)}$ *	25 ± 1 $^{(a)}$ *
		TM	21 ± 0 $^{(a)}$ *	23 ± 2 $^{(b)}$	20 ± 1 $^{(c)}$ *	22 ± 3 $^{(a,b,d)}$ *	20 ± 1 $^{(c,d)}$ *	22 ± 1 $^{(a,b)}$ *
	[Sn]	**DM**	2.9 ± 0.2 $^{(a)}$ *	2.3 ± 0.1 $^{(b)}$ *	2.5 ± 0.1 $^{(d)}$ *	2.9 ± 0.2 $^{(a)}$ *	2.8 ± 0.3 $^{(a)}$ *	3.4 ± 0.7 $^{(c)}$
		TM	2.1 ± 0.1 $^{(a)}$ *	2.1 ± 0.2 $^{(a,b)}$ *	2.1 ± 0.1 $^{(b)}$ *	2.3 ± 0.4 $^{(a,b)}$ *	3.1 ± 0.2 $^{(c)}$ *	3.6 ± 1.1 $^{(c)}$
	[Ti]	**DM**	1139 ± 55 $^{(a)}$ *	946 ± 76 $^{(b)}$ *	1040 ± 11 $^{(c)}$ *	1143 ± 12 $^{(a)}$ *	1186 ± 164 $^{(a)}$ *	1294 ± 327 $^{(a)}$ *
		TM	675 ± 23 $^{(a)}$ *	799 ± 28 $^{(b)}$ *	831 ± 39 $^{(c)}$ *	874 ± 132 $^{(b,c,d)}$ *	916 ± 122 $^{(d)}$ *	971 ± 67 $^{(d)}$ *
	[U]	**DM**	3.4 ± 0.4 $^{(a,c)}$ *	3.1 ± 0.2 $^{(a)}$ *	3,0 ± 0.1 $^{(b)}$ *	3.3 ± 0.0 $^{(c)}$ *	3.5 ± 0.2 $^{(c)}$ *	3.7 ± 0.4 $^{(c)}$ *
		TM	2.7 ± 0.2 $^{(a)}$ *	2.9 ± 0.1 $^{(b)}$ *	2.6 ± 0.1 $^{(c)}$ *	2.8 ± 0.4 $^{(a,b)}$ *	2.7 ± 0.4 $^{(a,b,c)}$ *	2.8 ± 0.0 $^{(a)}$ *
	[Zn]	**DM**	143 ± 15 $^{(a,c)}$	127 ± 2 $^{(b)}$ *	128 ± 4 $^{(b)}$ *	129 ± 4 $^{(b)}$ *	136 ± 3 $^{(c)}$ *	146 ± 11 $^{(a)}$
		TM	140 ± 3 $^{(a)}$	151 ± 3 $^{(b)}$ *	141 ± 7 $^{(a)}$ *	146 ± 14 $^{(a,b)}$ *	143 ± 8 $^{(a)}$ *	154 ± 9 $^{(b)}$

Table 2
Temperature (°C), light intensity (Lum m^{-2}) and total precipitation (mm) registered. Values are presented as means ± standard deviation.

	Temperature (°C)	Light Intensity (Lum m^{-2})	Total Precipitation (mm)
SUM 20	27 ± 3	23,030 ± 23,282	25 ± 22
AUT 20	19 ± 5	18,722 ± 17,470	132 ± 49
WIN 20	18 ± 5	10,043 ± 7499	88 ± 63
SPR 21	24 ± 4	11,318 ± 9663	68 ± 41
SUM 21	26 ± 3	22,183 ± 21,684	31 ± 32
AUT 21	19 ± 2	17,251 ± 7463	84 ± 44

limited to GPx, with higher activity in the TM meadow. Regarding temporal variations, significant differences were observed across all studied parameters, except for GST and GSSG in belowground tissue. The most pronounced variations in belowground tissues were seen in SOD, GPx, and GR activities (Fig. 3A, D, and 3G, respectively), with lower values during winter and higher values in spring and/or summer. In aboveground tissue, the most significant changes were observed in SOD, APX, GPx, GSH, GSSG, GR, and GST (Fig. 3A and 3C-H), with lower activities and levels during winter and higher values in summer and/or autumn.

Concerning oxidative damage, no significant differences between the DM and TM meadows were found for LPO and PC (Fig. 4). However, temporal variations were observed in both tissues. LPO levels were generally lower in winter and increased until late summer/autumn. In contrast, PC levels showed different patterns between aboveground and belowground tissues, with higher PC levels observed in belowground tissue during winter and lower levels in summer, whereas the opposite pattern was found in aboveground tissue.

4. Discussion

Based on the interpretation of sediment characterization data, seasonal climatic variations, and biochemical markers, it is possible to clarify plant acclimation during the early transplantation phase and its potential long-term adaptations to abiotic stressors.

4.1. Sediment characterization

The concentrations of metal(loid)s (As, Cd, Cu, Hg, and Zn) were significantly higher in the TM site, located near the contamination source, compared to the DM. This spatial gradient aligns with previous studies that demonstrate a decrease in metal(loid)s concentrations with increased distance from the source (Coelho et al., 2005; Ereira et al., 2015; Stoichev et al., 2019, 2020). Additionally, other elements analysed in this study correlated with geochemical variables such as fine sediment fraction, organic carbon, total carbon, and organic matter, consistent with the findings of Stoichev et al. (2020), suggesting that geochemical variables also play a role in the distribution of contaminants. Comparisons with earlier studies in the Aveiro lagoon indicate an overall decline in surface sediment contaminant levels over time (Ereira et al., 2015; García-Seoane et al., 2016; Oliveira et al., 2018), reinforcing the hypothesis of natural attenuation processes following the cessation of contaminant discharges, as there have been no active human remediation efforts in the region. Although variations over time were also noted, the temporal data dispersion suggests that these changes may partly be due to spatial variability and intrinsic sediment characteristics (e.g., fine fraction and organic matter content), rather than solely seasonal effects. These findings suggest that metal(loid) concentrations have remained relatively stable over the short period examined.

When comparing the observed metal(loid)s concentrations to the Probable Effect Level (PEL) values according to the Canadian standard for marine sediment quality (CCME, 2002), Hg is the only element that exceeded its reference threshold (PEL = 0.7 mg kg^{-1} dry weight) at the TM site. This finding suggests that, among the contaminants analysed, Hg is the most likely to exert adverse effects on both the seagrass and the local fauna. Since the other metal(loid)s remained below their respective PEL values, the ecological risk at this site appears to be primarily associated with Hg contamination.

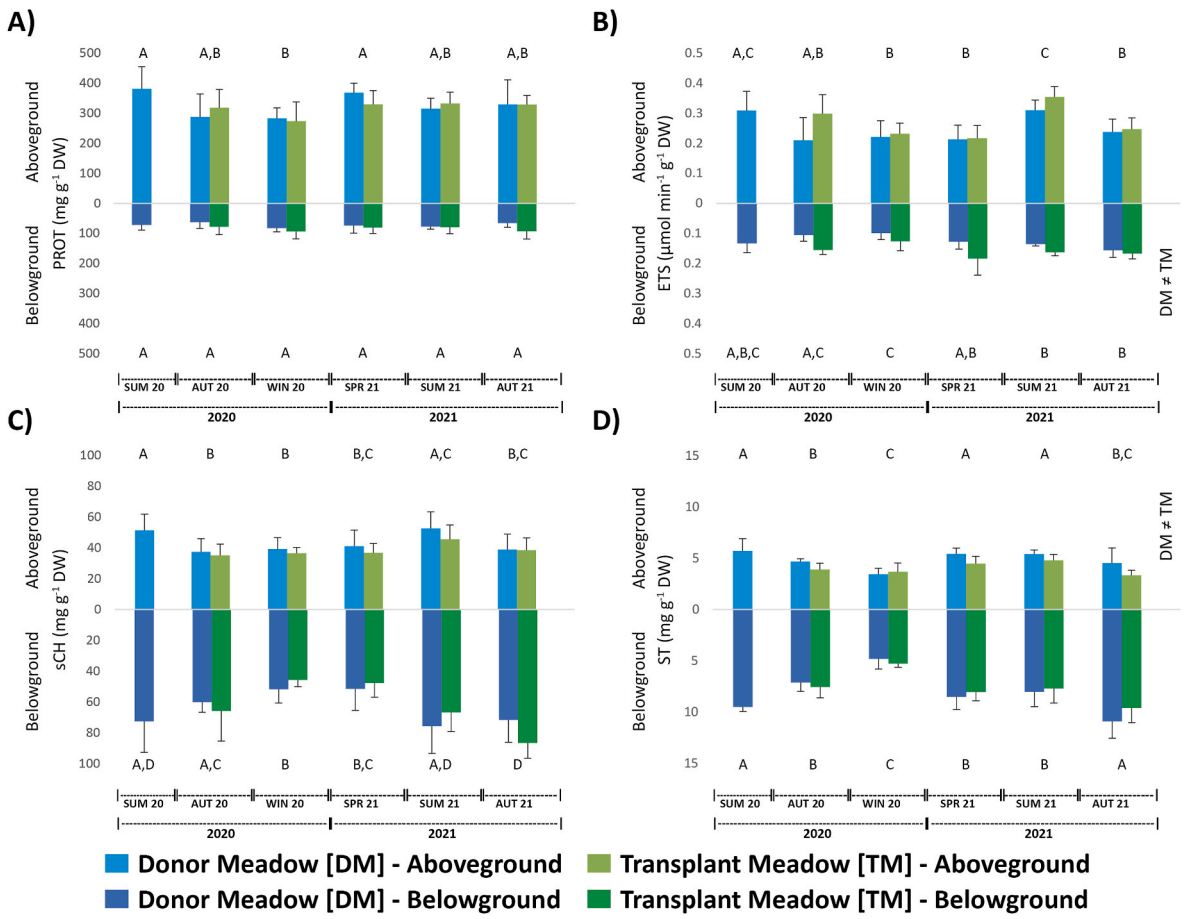

Fig. 2. Biochemical response in *Zostera noltei* (above and belowground tissues) over time at different sites (Donor Meadow and Transplant Meadow). (A) Soluble protein content [PROT]. (B) Electron transport system [ETS]. (C) Soluble carbohydrates [sCH]. (D) Starch [ST]. Columns represent the mean (n = 10), and error bars indicate the standard error. Different upper-case letters indicate significant differences between times ($p < 0.05$), while "DM ≠ TM" denotes significant differences between meadows for the specific tissue, when present.

4.2. Biochemical response of Zostera noltei

4.2.1. Adaptation to the early transplantation phase

In the initial stages following transplantation, when a direct comparison between TM and DM sites was possible (autumn 2020), *Zostera noltei* at the TM site exhibited pronounced biochemical changes. These changes highlight the plant's efforts to cope with two simultaneous stressors: the physical stress associated with transplantation and the initial exposure to contaminants, with Hg possibly exerting the most significant effect in this area.

Both aboveground and belowground tissues showed a significant increase in ETS activity, indicating an increased metabolic demand, likely serving as a compensatory response to stress (Bat et al., 2021; Malea et al., 1994; Rosalina et al., 2022). This enhanced ETS activity supports energy production and is coupled with the need to reestablish the root system after transplantation and with the upregulation of key antioxidant defence mechanisms, including enzymes such as SOD, CAT, and GPx, which are essential for scavenging ROS generated during transplantation to a metal contaminated area. Laboratory studies by Oliveira et al. (2025b) demonstrated that handling plants and disturbing sediment during transplantation can transiently boost ETS activity and cause membrane damage. However, these effects were observed only for a brief period (approximately 15 days), primarily due to temporary damage to the root system when patches were removed from Donor meadow, potentially resulting in injury or cutting of roots and rhizomes. A key parameter distinguishing this initial adaptation phase was the drastic reduction in GSH levels, most likely due to its rapid consumption during detoxification processes. GSH plays a central role in the GPx and APX cycles by converting hydrogen peroxide into water, a reaction that depletes available GSH under conditions of increased oxidative stress (Sofo et al., 2010).

Furthermore, a similar increase in SOD, GR, and GPx activity was observed when, for example, Hg, Cu, Cd, and Pb accumulation in seagrass tissues began to rise, as noted by Lin et al. (2016) and Oliveira et al. (2025b). Accordingly, these studies suggest that when metals start accumulating in plant tissues, these antioxidant enzymes become increasingly active and may also promote slight increases in membrane and protein damage. However, seagrass plants have the ability to subsequently develop defence mechanisms against contaminant absorption, such as releasing exudates to reduce metal(loid) bioavailability (Agarwal et al., 2024; Greco et al., 2019; Padmavathiamma and Li, 2012) or internal mechanisms, such as the production of phytochelatins, which bind to metal(loid)s, forming metal-phytochelatin complexes in vacuoles (Faizan et al., 2024; Li et al., 2023; Lima et al., 2012; Nguyen et al., 2017).

4.2.2. Adaptation over time

As the transplantation period extends, the continuous elevation of antioxidant enzymes and the development of additional defence mechanisms appear to lessen the differences between the TM and DM sites, particularly in terms of oxidative damage. This indicates that transplanted *Z. noltei* gradually achieves a new adaptive equilibrium, in which persistent metal-induced stress is effectively balanced by enhanced protective responses. Once this equilibrium is established, a

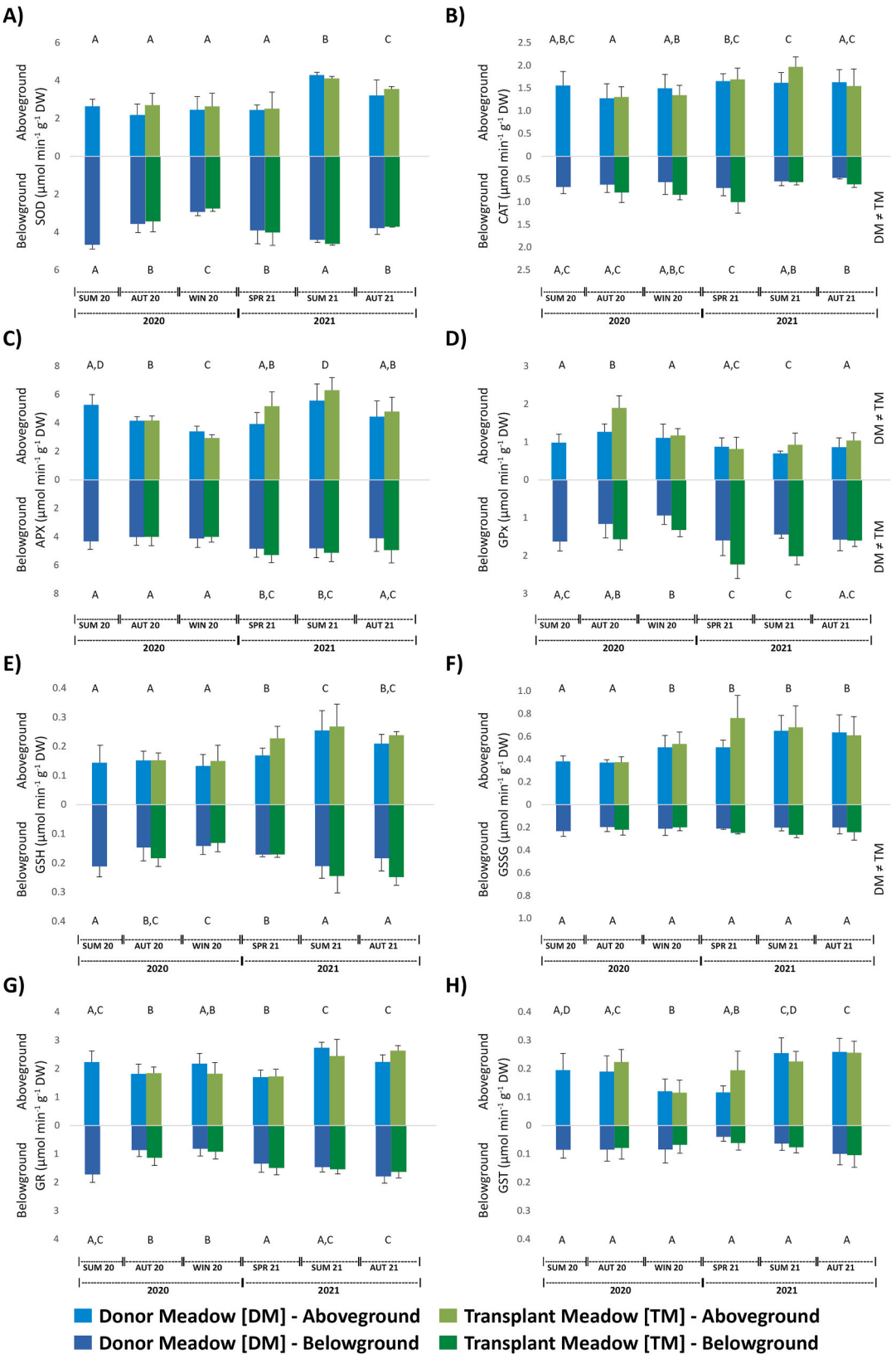

Fig. 3. Biochemical response in *Zostera noltei* (above and belowground tissues) over time at different sites (Donor Meadow and Transplant Meadow). (A) Superoxide dismutase [SOD]. (B) Catalase [CAT]. (C) Ascorbate peroxidase [APX]. (D) Glutathione peroxidase activity [GPx]. (E) Reduced glutathione [GSH]. (F) Glutathione oxidase [GSSG]. (G) Glutathione reductase [GR]. (H) Glutathione S-transferases activity [GST]. Columns represent the mean (n = 10), and error bars indicate the standard error. Different upper-case letters indicate significant differences between times ($p < 0.05$), while "DM ≠ TM" denotes significant differences between meadows for the specific tissue, when present.

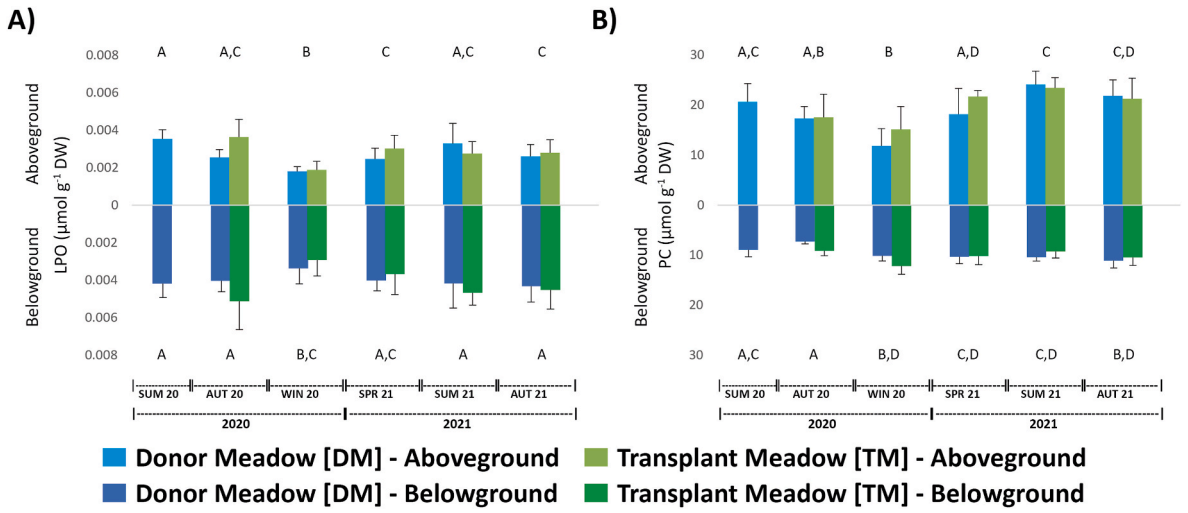

Fig. 4. Biochemical response in *Zostera noltei* (above and belowground tissues) over time at different sites (Donor Meadow and Transplant Meadow). (A) lipid peroxidation [LPO]. (B) Protein carbonylation [PC]. Columns represent the mean (n = 10), and error bars indicate the standard error. Different upper-case letters indicate significant differences between times ($p < 0.05$), while "DM ≠ TM" denotes significant differences between meadows for the specific tissue, when present.

distinct seasonal pattern emerges in the biochemical processes, influenced by environmental conditions and the plant's developmental cycle. For example, during winter, lower temperatures and reduced light intensity lead to diminished photosynthetic activity (Olivé et al., 2007), lower energy demands (Soissons et al., 2018), and consequently reduced ETS and antioxidant enzyme activities (Khan et al., 2021; Manara, 2012; Pereira et al., 2018). In contrast, the warmer seasons (spring and summer) promote higher photosynthetic rates and increased transpiration processes, which imply greater absorption of water and metal(loid)s in solution, enhanced carbohydrate production, and subsequently elevated ROS formation, which in turn stimulates the activity of CAT, APX, and GPx. The seasonal biochemical trends (increases and decreases) observed in this study coincide with biomass fluctuations (vegetative growth) reported by Oliveira et al. (2025a) and are consistent with both laboratory findings (Oliveira et al., 2025b) and studies on other seagrass species, such as *Enhalus acoroides*, *Thalassia hemprichii*, and *Cymodocea rotundata* (Govers et al., 2015; Olivé et al., 2007; Ouisse et al., 2010; Soissons et al., 2018; Vermaat and Verhagen, 1996; Zhang et al., 2022). Although the continued presence of contaminants maintains higher antioxidant enzymatic activity in transplanted plants relative to those in the Donor meadow, laboratory experiments conducted by Fonte et al. (2023) and Oliveira et al. (2025b), indicate that *Z. noltei* can tolerate Hg and other metal(loid)s (As, Cd, Cu, and Zn) at concentrations far exceeding those currently observed at the transplantation site. The precise upper limit at which these defence mechanisms might be overwhelmed, however, remains to be determined.

5. Conclusion

Integrating sediment and biochemical data demonstrates that *Z. noltei* employs a coherent adaptive strategy in response to environmental stress. Elevated contaminant levels, primarily Hg, at the transplant site, combined with the transplantation process, trigger an immediate upregulation of ETS and antioxidant enzymes as an acute response to the new conditions. Over time, the plant achieves a new adaptive equilibrium through inducible defence mechanisms and physiological adjustments, with seasonal factors such as temperature, light intensity, contaminant accumulation, and vegetative growth further modulating these responses. Overall, these insights not only underscore the resilience and acclimatization potential of *Z. noltei* but also enable early detection of maladaptation, thereby facilitating timely interventions to enhance the long-term success of restoration projects in contaminated ecosystems.

CRediT authorship contribution statement

V.H. Oliveira: Writing – review & editing, Writing – original draft, Visualization, Validation, Methodology, Investigation, Formal analysis, Data curation, Conceptualization. **D. Matos:** Writing – review & editing, Investigation. **A.I. Sousa:** Writing – review & editing, Resources, Methodology, Investigation, Formal analysis. **M. Dolbeth:** Writing – review & editing, Investigation, Formal analysis. **B. Marques:** Investigation. **A.I. Lillebø:** Writing – review & editing, Resources. **M.E. Pereira:** Writing – review & editing, Resources. **S. Díez:** Writing – review & editing, Resources. **E. Figueira:** Writing – review & editing, Resources. **J.P. Coelho:** Writing – review & editing, Supervision, Resources, Project administration, Methodology, Investigation, Funding acquisition, Formal analysis, Conceptualization.

Declaration of Generative AI and AI-assisted technologies in the writing process

During the preparation of this work, the author(s) used ChatGPT in order to improve the language and readability of manuscript. After using this tool/service, the author(s) reviewed and edited the content as needed and take(s) full responsibility for the content of the publication.

Declaration of competing interest

The authors declare that they have no known competing financial interests or personal relationships that could have appeared to influence the work reported in this paper.

Acknowledgements

The authors acknowledge FCT – Foundation for Science and Technology for the PhD grant of Vitor Oliveira (reference 2020.04621.BD and DOI 10.54499/2020.04621.BD) and Diana Matos (reference 2020.07142.BD and DOI 10.54499/2020.07142.BD) and the research contracts of João P. Coelho (reference 2020.01778.CEECIND/CP1589/CT0011 and DOI 10.54499/2020.01778.CEECIND/CP1589/CT0011), Marina Dolbeth (reference CEECINST/00027/2021/CP2789/CT0001 and DOI 10.54499/CEECINST/00027/2021/CP2789/CT0001) and Ana I. Sousa (reference CEECIND/00962/2017/CP1459/CT0008 and DOI 10.54499/CEECIND/00962/2017/CP1459/CT0008)

This work was partially funded by project RemediGrass (PTDC/CTA-AMB/29647/2017) funded by FEDER, through COMPETE2020 -

Programa Operacional Competitividade e Internacionalização (POCI), and by national funds (OE), through FCT/MCTES (Fundação para a Ciência e Tecnologia and Ministério da Ciência, Tecnologia e Ensino Superior) and Horizon Europe RESTORE4Cs project, funded by the European Commission (Grant agreement ID: 101056782; 10.3030/101056782). Thanks are also due to FCT/MCTES for the financial support to UID Centro de Estudos do Ambiente e Mar (CESAM) + LA/P/0094/2020, REQUIMTE (UIDB/50006/2020 and UIDP/50006/2020), and CIIMAR (UIDB/04423/2020 and UIDP/04423/2020), through national funds.

Appendix A. Supplementary data

Supplementary data to this article can be found online at https://doi.org/10.1016/j.jenvman.2025.124918.

Data availability

Data will be made available on request.

References

Agarwal, P., Vibhandik, R., Agrahari, R., Daverey, A., Rani, R., 2024. Role of root exudates on the soil microbial diversity and biogeochemistry of heavy metals. Appl. Biochem. Biotechnol. 196, 2673–2693. https://doi.org/10.1007/s12010-023-04465-2.

Anderson, M., Gorley, R.N., Clarke, K., 2008. PERMANOVA+ for Primer: Guide to Software and Statistical Methods. Primer-E, Plymouth. https://learninghub.primer-e.com/books/permanova-for-primer-guide-to-software-and-statistical-methods.

Bashir, I., Lone, F.A., Bhat, R.A., Mir, S.A., Dar, Z.A., Dar, S.A., 2020. Concerns and threats of contamination on aquatic ecosystems. In: Bioremediation and Biotechnology. Springer International Publishing, Cham, pp. 1–26. https://doi.org/10.1007/978-3-030-35691-0_1.

Bat, L., Arici, E., Öztekin, A., 2021. Threats to quality in the coasts of the black sea: heavy metal pollution of seawater, sediment, macro-algae and seagrass. In: Shit, P.K, Adhikary, P.P., Sengupta, D. (Eds.), Spatial Modeling and Assessment of Environmental Contaminants. Environmental Challenges and Solutions. Springer, Cham, pp. 289–325. https://doi.org/10.1007/978-3-030-63422-3_18.

Beauchamp, C., Fridovich, I., 1971. Superoxide dismutase: improved assays and an assay applicable to acrylamide gels. Anal. Biochem. 44, 276–287. https://doi.org/10.1016/0003-2697(71)90370-8.

Beaumont, N.J., Austen, M.C., Atkins, J.P., Burdon, D., Degraer, S., Dentinho, T.P., Derous, S., Holm, P., Horton, T., van Ierland, E., Marboe, A.H., Starkey, D.J., Townsend, M., Zarzycki, T., 2007. Identification, definition and quantification of goods and services provided by marine biodiversity: implications for the ecosystem approach. Mar. Pollut. Bull. 54, 253–265. https://doi.org/10.1016/j.marpolbul.2006.12.003.

Blanco-Murillo, F., Marín-Guirao, L., Sola, I., Carbonell-Garzón, E., Rodríguez-Rojas, F., Sánchez-Lizaso, J.L., Sáez, C.A., 2024. Metabolic responses to desalination brine discharges in field-transplanted Posidonia oceanica: advances for the development of specific early warning biomarkers. Desalination 576, 117395. https://doi.org/10.1016/j.desal.2024.117395.

Bonanno, G., Orlando-Bonaca, M., 2017. Trace elements in Mediterranean seagrasses: accumulation, tolerance and biomonitoring. A review. Mar. Pollut. Bull. 125, 8–18. https://doi.org/10.1016/j.marpolbul.2017.10.078.

Brackup, I., Capone, D.G., 1985. The effect of several metal and organic pollutants on nitrogen fixation (acetylene reduction) by the roots and rhizomes of Zostera marina L. Environ. Exp. Bot. 25, 145–151. https://doi.org/10.1016/0098-8472(85)90020-6.

Brix, H., Lyngby, J.E., Schierup, H.-H., 1983. Eelgrass (Zostera marina L.) as an indicator organism of trace metals in the Limfjord, Denmark. Mar. Environ. Res. 8, 165–181. https://doi.org/10.1016/0141-1136(83)90049-1.

Brown, C.J., Adame, M.F., Buelow, C.A., Frassl, M.A., Lee, S.Y., Mackey, B., McClure, E. C., Pearson, R.M., Rajkaran, A., Rayner, T.S., Sievers, M., Saint Ange, C.A., Sousa, A. I., Tulloch, V.J.D., Turschwell, M.P., Connolly, R.M., 2021. Opportunities for improving recognition of coastal wetlands in global ecosystem assessment frameworks. Ecol. Indic. 126, 107694. https://doi.org/10.1016/j.ecolind.2021.107694.

Brun, F.G., Cobo-Díaz, J.F., González-Ortiz, V., Varela, J.L., Pérez-Lloréns, J.L., Vergara, J.J., 2021. Seagrass patch complexity affects macroinfaunal community structure in intertidal areas: an in situ experiment using seagrass mimics. Diversity 13, 572. https://doi.org/10.3390/d13110572.

Buapet, P., Mohammadi, N.S., Pernice, M., Kumar, M., Kuzhiumparambil, U., Ralph, P.J., 2019. Excess copper promotes photoinhibition and modulates the expression of antioxidant-related genes in Zostera muelleri. Aquat. Toxicol. 207, 91–100. https://doi.org/10.1016/j.aquatox.2018.12.005.

Buege, J.A., Aust, S.D., 1978. [30] Microsomal lipid peroxidation 302–310. https://doi.org/10.1016/S0076-6879(78)52032-6.

Carlberg, I., Mannervik, B., 1985. [59] Glutathione reductase 484–490. https://doi.org/10.1016/S0076-6879(85)13062-4.

CCME, 2002. Canadian sediment quality guidelines for the protection of aquatic life. https://ccme.ca/en/current-activities/canadian-environmental-quality-guidelines.

Chen, S., Qiu, G., 2024. Physiological and multi-omics analysis reveals the influence of copper on Halophila beccarii Asch. Plant Physiol. Biochem. 212, 108785. https://doi.org/10.1016/j.plaphy.2024.108785.

Coelho, J.P., Pereira, M.E., Duarte, A., Pardal, M.A., 2005. Macroalgae response to a mercury contamination gradient in a temperate coastal lagoon (Ria de Aveiro, Portugal). Estuar. Coast Shelf Sci. 65, 492–500. https://doi.org/10.1016/j.ecss.2005.06.020.

Costa, V., Flindt, M.R., Lopes, M., Coelho, J.P., Costa, A.F., Lillebø, A.I., Sousa, A.I., 2022. Enhancing the resilience of Zostera noltei seagrass meadows against Arenicola spp. bio-invasion: a decision-making approach. J. Environ. Manag. 302, 113969. https://doi.org/10.1016/j.jenvman.2021.113969.

Costley, C.T., Mossop, K.F., Dean, J.R., Garden, L.M., Marshall, J., Carroll, J., 2000. Determination of mercury in environmental and biological samples using pyrolysis atomic absorption spectrometry with gold amalgamation. Anal. Chim. Acta 405, 179–183. https://doi.org/10.1016/S0003-2670(99)00742-4.

Crespo, D., Faião, R., Freitas, V., Oliveira, V.H., Sousa, A.I., Coelho, J.P., Dolbeth, M., 2023. Using seagrass as a nature-based solution: short-term effects of Zostera noltei transplant in benthic communities of a European Atlantic coastal lagoon. Mar. Pollut. Bull. 197, 115762. https://doi.org/10.1016/j.marpolbul.2023.115762.

De Coen, W.M., Janssen, C.R., 1997. The use of biomarkers in Daphnia magna toxicity testing. IV. Cellular Energy Allocation: a new methodology to assess the energy budget of toxicant-stressed Daphnia populations. J. Aquatic Ecosyst. Stress Recovery 6, 43–55. https://doi.org/10.1023/A:1008228517955.

DuBois, M., Gilles, K.A., Hamilton, J.K., Rebers, P.A., Smith, F., 1956. Colorimetric method for determination of sugars and related substances. Anal. Chem. 28, 350–356. https://doi.org/10.1021/ac60111a017.

Ereira, T., Coelho, J.P., Duarte, A.C., Pardal, M.A., Pereira, M.E., 2015. Size-Dependent Arsenic Accumulation in Scrobicularia plana in a Temperate Coastal Lagoon (Ria de Aveiro, Portugal). Water Air Soil Pollut. 226, 213. https://doi.org/10.1007/s11270-015-2484-5.

Faizan, M., Alam, P., Hussain, A., Karabulut, F., Tonny, S.H., Cheng, S.H., Yusuf, M., Adil, M.F., Sehar, S., Alomrani, S.O., Albalawi, T., Hayat, S., 2024. Phytochelatins: key regulator against heavy metal toxicity in plants. Plant Stress 11, 100355. https://doi.org/10.1016/j.stress.2024.100355.

Figueira, E., Freitas, R., Pereira, E., Duarte, A., 2012. Mercury uptake and allocation in Juncus maritimus: implications for phytoremediation and restoration of a mercury contaminated salt marsh. J. Environ. Monit. 14, 2181. https://doi.org/10.1039/c2em30076a.

Fonte, B.A., Oliveira, V.H., Sousa, A.I., Lopes, C.B., Henriques, B., Pereira, M.E., Figueira, E., Calado, R., Lillebø, A.I., Coelho, J.P., 2023. Zostera noltei response to transplantation into historically Hg-contaminated sediments (A mesocosm experiment): growth, bioaccumulation and photosynthetic performance. Chemosphere 337, 139374. https://doi.org/10.1016/j.chemosphere.2023.139374.

García-Seoane, E., Coelho, J.P., Mieiro, C., Dolbeth, M., Ereira, T., Rebelo, J.E., Pereira, E., 2016. Effect of historical contamination in the fish community structure of a recovering temperate coastal lagoon. Mar. Pollut. Bull. 111, 221–230. https://doi.org/10.1016/j.marpolbul.2016.07.005.

Govers, L.L., Suykerbuyk, W., Hoppenreijs, J.H.T., Giesen, K., Bouma, T.J., van Katwijk, M.M., 2015. Rhizome starch as indicator for temperate seagrass winter survival. Ecol. Indic. 49, 53–60. https://doi.org/10.1016/j.ecolind.2014.10.002.

Greco, M., Sáez, C.A., Contreras, R.A., Rodríguez-Rojas, F., Bitonti, M.B., Brown, M.T., 2019. Cadmium and/or copper excess induce interdependent metal accumulation, DNA methylation, induction of metal chelators and antioxidant defences in the seagrass Zostera marina. Chemosphere 224, 111–119. https://doi.org/10.1016/j.chemosphere.2019.02.123.

Griffiths, L.L., Melvin, S.D., Connolly, R.M., Pearson, R.M., Brown, C.J., 2020. Metabolomic indicators for low-light stress in seagrass. Ecol. Indic. 114, 106316. https://doi.org/10.1016/j.ecolind.2020.106316.

Habig, W.H., Pabst, M.J., Jakoby, W.B., 1974. Glutathione S-transferases. J. Biol. Chem. 249, 7130–7139. https://doi.org/10.1016/S0021-9258(19)42083-8.

Hamad, A.A., Moubasher, H.A., Moustafa, Y.M., Mohamed, N.H., Abd-el rhim, E.H., 2021. Petroleum hydrocarbon bioremediation using native fungal isolates and consortia. Sci. World J. 1–13. https://doi.org/10.1155/2021/6641533, 2021.

Jiménez-Ramos, R., Egea, L.G., Vergara, J.J., Bouma, T.J., Brun, F.G., 2019. The role of flow velocity combined with habitat complexity as a top–down regulator in seagrass meadows. Oikos 128, 64–76. https://doi.org/10.1111/oik.05452.

Johansson, L.H., Håkan Borg, L.A., 1988. A spectrophotometric method for determination of catalase activity in small tissue samples. Anal. Biochem. 174, 331–336. https://doi.org/10.1016/0003-2697(88)90554-4.

Kang, B., Pecl, G.T., Lin, L., Sun, P., Zhang, P., Li, Y., Zhao, L., Peng, X., Yan, Y., Shen, C., Niu, W., 2021. Climate change impacts on China's marine ecosystems. Rev. Fish Biol. Fish. 31, 599–629. https://doi.org/10.1007/s11160-021-09668-6.

Karimi, H., Mahdavi, S., Asgari Lajayer, B., Moghiseh, E., Rajput, V.D., Minkina, T., Astatkie, T., 2022. Insights on the bioremediation technologies for pesticide-contaminated soils. Environ. Geochem. Health 44, 1329–1354. https://doi.org/10.1007/s10653-021-01081-z.

Kerninon, F., Payri, C.E., Le Loc'h, F., Alcoverro, T., Maréchal, J.-P., Chalifour, J., Gréaux, S., Mège, S., Athanase, J., Cordonnier, S., Rouget, M.-L., Lorre, E., Uboldi, T., Monnier, O., Hellio, C., 2021. Selection of parameters for seagrass management: towards the development of integrated indicators for French Antilles. Mar. Pollut. Bull. 170, 112646. https://doi.org/10.1016/j.marpolbul.2021.112646.

Khan, I., Awan, S.A., Rizwan, M., Ali, S., Hassan, M.J., Brestic, M., Zhang, X., Huang, L., 2021. Effects of silicon on heavy metal uptake at the soil-plant interphase: a review.

Ecotoxicol. Environ. Saf. 222, 112510. https://doi.org/10.1016/j.ecoenv.2021.112510.
Lee, G., Suonan, Z., Kim, S.H., Hwang, D.-W., Lee, K.-S., 2019. Heavy metal accumulation and phytoremediation potential by transplants of the seagrass Zostera marina in the polluted bay systems. Mar. Pollut. Bull. 149, 110509. https://doi.org/10.1016/j.marpolbul.2019.110509.
Li, Y., Chen, F., Zhou, R., Zheng, X., Pan, K., Qiu, G., Wu, Z., Chen, S., Wang, D., 2023. A review of metal contamination in seagrasses with an emphasis on metal kinetics and detoxification. J. Hazard Mater. 454, 131500. https://doi.org/10.1016/j.jhazmat.2023.131500.
Lima, A.I.G., Da Cruz e Silva, E., Figueira, E.M.P.A., 2012. Cd-induced signaling pathways in plants: possible regulation of PC synthase by protein phosphatase 1. Environ. Exp. Bot. 79, 31–36. https://doi.org/10.1016/j.envexpbot.2011.12.036.
Lin, H., Sun, T., Zhou, Y., Zhang, X., 2016. Anti-oxidative feedback and biomarkers in the intertidal seagrass Zostera japonica induced by exposure to copper, lead and cadmium. Mar. Pollut. Bull. 109, 325–333. https://doi.org/10.1016/j.marpolbul.2016.05.062.
Malea, P., Haritonidis, S., Kevrekidis, T., 1994. Seasonal and local variations of metal concentrations in the seagrass Posidonia oceanica (L.) Delile in the Antikyra Gulf, Greece. Sci. Total Environ. 153, 225–235. https://doi.org/10.1016/0048-9697(94)90202-X.
Manara, A., 2012. Plant Responses to Heavy Metal Toxicity 27–53. https://doi.org/10.1007/978-94-007-4441-7_2.
Morris, E.P., Peralta, G., Brun, F.G., van Duren, L., Bouma, T.J., Perez-Llorens, J.L., 2008. Interaction between hydrodynamics and seagrass canopy structure: spatially explicit effects on ammonium uptake rates. Limnol. Oceanogr. 53, 1531–1539. https://doi.org/10.4319/lo.2008.53.4.1531.
Nakano, Y., Asada, K., Nakano, Y., Asada, K., 1981. Hydrogen peroxide is scavenged by ascorbate-specific peroxidase in spinach chloroplasts. Plant Cell Physiol. 22, 867–880. https://doi.org/10.1093/oxfordjournals.pcp.a076232.
Nguyen, X.-V., Le-Ho, K.-H., Papenbrock, J., 2017. Phytochelatin 2 accumulates in roots of the seagrass Enhalus acoroides collected from sediment highly contaminated with lead. Biometals 30, 249–260. https://doi.org/10.1007/s10534-017-9998-9.
Nunes, M., Coelho, J.P., Cardoso, P.G., Pereira, M.E., Duarte, A.C., Pardal, M.A., 2008. The macrobenthic community along a mercury contamination in a temperate estuarine system (Ria de Aveiro, Portugal). Sci. Total Environ. 405, 186–194. https://doi.org/10.1016/j.scitotenv.2008.07.009.
Olivé, I., Brun, F.G., Vergara, J.J., Pérez-Lloréns, J.L., 2007. Effects of light and biomass partitioning on growth, photosynthesis and carbohydrate content of the seagrass Zostera noltii Hornem. J. Exp. Mar. Biol. Ecol. 345, 90–100. https://doi.org/10.1016/j.jembe.2007.02.008.
Oliveira, V.H., Coelho, J.P., Borgogni, R., Pereira, M.E., Figueira, E., 2022. Metal(oid)s accumulation (Hg and As) and their biochemical effects in Halimione portulacoides (Ria de Aveiro, Portugal). Mar. Pollut. Bull. 180, 113804. https://doi.org/10.1016/j.marpolbul.2022.113804.
Oliveira, V.H., Coelho, J.P., Reis, A.T., Vale, C., Bernardes, C., Pereira, M.E., 2018. Mobility versus retention of mercury in bare and salt marsh sediments of a recovering coastal lagoon (Ria de Aveiro, Portugal). Mar. Pollut. Bull. 135, 249–255. https://doi.org/10.1016/j.marpolbul.2018.07.035.
Oliveira, V.H., Díez, S., Dolbeth, M., Coelho, J.P., 2024. Restoration of degraded estuarine and marine ecosystems: a systematic review of rehabilitation methods in Europe. J. Hazard Mater. 469, 133863. https://doi.org/10.1016/j.jhazmat.2024.133863.
Oliveira, V.H., Fonte, B.A., Sousa, A.I., Crespo, D., Dias, J.M., Vaz, N., Matos, D., Figueira, E., Pereira, M.E., Lillebø, A.I., Dolbeth, M., Coelho, J.P., 2025a. Transplantation of seagrass (Zostera noltei) as a potential nature-based solution for the restoration of historically contaminated mudflats. Sci. Total Environ. 959, 178257. https://doi.org/10.1016/j.scitotenv.2024.178257.
Oliveira, V.H., Fonte, B.A., Costa, F., Sousa, A.I., Henriques, B., Pereira, E., Dolbeth, M., Díez, S., Coelho, J.P., 2023. The effect of Zostera noltei recolonization on the sediment mercury vertical profiles of a recovering coastal lagoon. Chemosphere 345, 140438. https://doi.org/10.1016/j.chemosphere.2023.140438.
Oliveira, V.H., Fonte, B.A., Sousa, A.I., Marques, B., Matos, D., Henriques, B., Pereira, M.E., Lopes, C.B., Calado, R., Lillebø, A.I., Figueira, E., Coelho, J.P., 2025b. Seagrass biochemical response to transplantation into contaminated sediments: A mesocosm experiment. Environ. Res. 121353. https://doi.org/10.1016/j.envres.2025.121353.
Orth, R.J., Lefcheck, J.S., McGlathery, K.S., Aoki, L., Luckenbach, M.W., Moore, K.A., Oreska, M.P.J., Snyder, R., Wilcox, D.J., Lusk, B., 2020. Restoration of seagrass habitat leads to rapid recovery of coastal ecosystem services. Sci. Adv. 6. https://doi.org/10.1126/sciadv.abc6434.
Ouisse, V., Migné, A., Davoult, D., 2010. Seasonal variations of community production, respiration and biomass of different primary producers in an intertidal Zostera noltii bed (Western English Channel, France). Hydrobiologia 649, 3–11. https://doi.org/10.1007/s10750-010-0254-3.
Padmavathiamma, P.K., Li, L.Y., 2012. Rhizosphere influence and seasonal impact on phytostabilisation of metals—a field study. Water Air Soil Pollut. 223, 107–124. https://doi.org/10.1007/s11270-011-0843-4.
Paglia, D.E., Valentine, W.N., 1967. Studies on the quantitative and qualitative characterization of erythrocyte glutathione peroxidase. J. Lab. Clin. Med. 70, 158–169.
Pereira, A.S., Dorneles, A.O.S., Bernardy, K., Sasso, V.M., Bernardy, D., Possebom, G., Rossato, L.V., Dressler, V.L., Tabaldi, L.A., 2018. Selenium and silicon reduce cadmium uptake and mitigate cadmium toxicity in Pfaffia glomerata (Spreng.) Pedersen plants by activation antioxidant enzyme system. Environ. Sci. Pollut. Res. 25, 18548–18558. https://doi.org/10.1007/s11356-018-2005-3.
Piro, A., Marín-Guirao, L., Serra, I.A., Spadafora, A., Sandoval-Gil, J.M., Bernardeau-Esteller, J., Fernandez, J.M.R., Mazzuca, S., 2015. The modulation of leaf metabolism plays a role in salt tolerance of Cymodocea nodosa exposed to hypersaline stress in mesocosms. Front. Plant Sci. 6. https://doi.org/10.3389/fpls.2015.00464.
Rahman, I., Kode, A., Biswas, S.K., 2007. Assay for quantitative determination of glutathione and glutathione disulfide levels using enzymatic recycling method. Nat. Protoc. 1, 3159.
Robinson, H.W., Hogden, C.G., 1940. The biuret reaction in the determination of serum proteins. J. Biol. Chem. 135, 727–731. https://doi.org/10.1016/S0021-9258(18)73135-9.
Rosalina, D., Rombe, K.H., Jamil, K., Surachmat, A., 2022. Analysis of heavy metals (Pb and Cd) in seagrasses Thalassia hemprichii and Enhalus acoroides from pulau sembilan, south Sulawesi Province, Indonesia. Biodiversitas J. Biol. Divers. 23. https://doi.org/10.13057/biodiv/d230448.
Rostami, S., Azhdarpoor, A., 2019. The application of plant growth regulators to improve phytoremediation of contaminated soils: a review. Chemosphere 220, 818–827. https://doi.org/10.1016/j.chemosphere.2018.12.203.
Salinas, C., Duarte, C.M., Lavery, P.S., Masque, P., Arias-Ortiz, A., Leon, J.X., Callaghan, D., Kendrick, G.A., Serrano, O., 2020. Seagrass losses since mid-20th century fuelled CO 2 emissions from soil carbon stocks. Glob. Change Biol. 26, 4772–4784. https://doi.org/10.1111/gcb.15204.
Sandoval-Gil, J.M., Ruiz, J.M., Marín-Guirao, L., 2023. Advances in understanding multilevel responses of seagrasses to hypersalinity. Mar. Environ. Res. 183, 105809. https://doi.org/10.1016/j.marenvres.2022.105809.
Sofo, A., Cicco, N., Paraggio, M., Scopa, A., 2010. Regulation of the ascorbate–glutathione cycle in plants under drought stress. In: Ascorbate-Glutathione Pathway and Stress Tolerance in Plants. Springer, Netherlands, Dordrecht, pp. 137–189. https://doi.org/10.1007/978-90-481-9404-9_5.
Soissons, L.M., Haanstra, E.P., van Katwijk, M.M., Asmus, R., Auby, I., Barillé, L., Brun, F.G., Cardoso, P.G., Desroy, N., Fournier, J., Ganthy, F., Garmendia, J.-M., Godet, L., Grilo, T.F., Kadel, P., Ondiviela, B., Peralta, G., Puente, A., Recio, M., Rigouin, L., Valle, M., Herman, P.M.J., Bouma, T.J., 2018. Latitudinal patterns in European seagrass carbon reserves: influence of seasonal fluctuations versus short-term stress and disturbance events. Front. Plant Sci. 9. https://doi.org/10.3389/fpls.2018.00088.
Sousa, A.I., Santos, D.B., Silva, E.F. da, Sousa, L.P., Cleary, D.F.R., Soares, A.M.V.M., Lillebø, A.I., 2017. 'Blue Carbon' and Nutrient Stocks of Salt Marshes at a Temperate Coastal Lagoon (Ria de Aveiro, Portugal). Sci. Rep. 7, 41225. https://doi.org/10.1038/srep41225.
Stoichev, T., Coelho, J.P., De Diego, A., Valenzuela, M.G.L., Pereira, M.E., de Chanvalon, A.T., Amouroux, D., 2020. Multiple regression analysis to assess the contamination with metals and metalloids in surface sediments (Aveiro Lagoon, Portugal). Mar. Pollut. Bull. 159, 111470. https://doi.org/10.1016/j.marpolbul.2020.111470.
Stoichev, T., Tessier, E., Coelho, J.P., Lobos Valenzuela, M.G., Pereira, M.E., Amouroux, D., 2019. Multiple regression analysis to assess the spatial distribution and speciation of mercury in surface sediments of a contaminated lagoon. J. Hazard Mater. 367, 715–724. https://doi.org/10.1016/j.jhazmat.2018.12.109.
Touchette, B.W., Burkholder, J.M., 2000. Overview of the physiological ecology of carbon metabolism in seagrasses. J. Exp. Mar. Biol. Ecol. 250, 169–205. https://doi.org/10.1016/S0022-0981(00)00196-9.
Udenigwe, C.C., Udechukwu, M.C., Yiridoe, C., Gibson, A., Gong, M., 2016. Antioxidant mechanism of potato protein hydrolysates against in vitro oxidation of reduced glutathione. J. Funct.Foods 20, 195–203. https://doi.org/10.1016/j.jff.2015.11.004.
Unsworth, R.K.F., Cullen-Unsworth, L.C., Jones, B.L.H., Lilley, R.J., 2022. The planetary role of seagrass conservation. Science 377, 609–613. https://doi.org/10.1126/science.abq6923.
Valdez, S.R., Zhang, Y.S., van der Heide, T., Vanderklift, M.A., Tarquinio, F., Orth, R.J., Silliman, B.R., 2020. Positive ecological interactions and the success of seagrass restoration. Front. Mar. Sci. 7. https://doi.org/10.3389/fmars.2020.00091.
Válega, M., Lillebø, A.I., Caçador, I., Pereira, M.E., Duarte, A.C., Pardal, M.A., 2008a. Mercury mobility in a salt marsh colonised by Halimione portulacoides. Chemosphere 72, 1607–1613. https://doi.org/10.1016/j.chemosphere.2008.04.007.
Válega, M., Lillebø, A.I., Pereira, M.E., Duarte, A.C., Pardal, M.A., 2008b. Long-term effects of mercury in a salt marsh: hysteresis in the distribution of vegetation following recovery from contamination. Chemosphere 71, 765–772. https://doi.org/10.1016/j.chemosphere.2007.10.013.
Verduin, J.J., Backhaus, J.O., 2000. Dynamics of plant–flow interactions for the seagrass amphibolis Antarctica: field observations and model simulations. Estuar. Coast Shelf Sci. 50, 185–204. https://doi.org/10.1006/ecss.1999.0567.
Vermaat, J.E., Verhagen, F.C.A., 1996. Seasonal variation in the intertidal seagrass Zostera noltii Hornem.: coupling demographic and physiological patterns. Aquat. Bot. 52, 259–281. https://doi.org/10.1016/0304-3770(95)00510-2.
Vishwakarma, G.S., Bhattacharjee, G., Gohil, N., Singh, V., 2020. Current status, challenges and future of bioremediation. In: Bioremediation of Pollutants. Elsevier, pp. 403–415. https://doi.org/10.1016/B978-0-12-819025-8.00020-X.
Wahyudi, A.J., Rahmawati, S., Irawan, A., Hadiyanto, H., Prayudha, B., Hafizt, M., Afdal, A., Adi, N.S., Rustam, A., Hernawan, U.E., Rahayu, Y.P., Iswari, M.Y., Supriyadi, I.H., Solihudin, T., Ati, R.N.A., Kepel, T.L., Kusumaningtyas, M.A., Daulat, A., Salim, H.L., Sudirman, N., Suryono, D.D., Kiswara, W., 2020. Assessing carbon stock and sequestration of the tropical seagrass meadows in Indonesia. Ocean Sci. J. 55, 85–97. https://doi.org/10.1007/s12601-020-0003-0.
Zhai, T., Wang, J., Fang, Y., Qin, Y., Huang, L., Chen, Y., 2020. Assessing ecological risks caused by human activities in rapid urbanization coastal areas: towards an

integrated approach to determining key areas of terrestrial-oceanic ecosystems preservation and restoration. Sci. Total Environ. 708, 135153. https://doi.org/10.1016/j.scitotenv.2019.135153.

Zhang, H., Yuan, X., Xiong, T., Wang, H., Jiang, L., 2020. Bioremediation of co-contaminated soil with heavy metals and pesticides: influence factors, mechanisms and evaluation methods. Chem. Eng. J. 398, 125657. https://doi.org/10.1016/j.cej.2020.125657.

Zhang, M., Zhang, L., Li, H., Liu, J., 2022. The lack of low temperature tolerance of tropical seagrasses strongly restricts their geographical distribution. Mar. Environ. Res. 173, 105539. https://doi.org/10.1016/j.marenvres.2021.105539.